Astron. Astrophys. 337, 797–807 (1998)

ASTRONOMY AND ASTROPHYSICS

CO observations and mass loss of MS- and S-stars⋆

M.A.T. Groenewegen[1] **and T. de Jong**[2,3]

[1] Max-Planck-Institut für Astrophysik, Karl-Schwarzschild-Straße 1, D-85740 Garching, Germany
[2] Astronomical Institute, Kruislaan 403, 1098 SJ Amsterdam, The Netherlands
[3] Space Research Organisation Netherlands, Sorbonnelaan 2, 3584 CA Utrecht, The Netherlands

Received 7 April 1998 / Accepted 3 June 1998

Abstract. We present ^{12}CO J = 1-0 and 2-1 observations of 14 S-stars, and report 6 new detections. Two stars were observed in the ^{13}CO J = 1-0 and 2-1 lines, and one tentative 2-1 detection is reported.

A compilation is presented of all CO observations of S-stars. The stars in this sample are separated into "intrinsic" and "extrinsic" S-stars, based on direct observation of the Technetium line, or infrared properties.

The dust mass loss rate per unit distance is derived from IRAS 60 μm data taking into the fact that for small mass loss rates the observed flux is an overestimate of the excess emission due to dust. The gas mass loss rate per unit distance is derived from CO data. Distances and luminosities are estimated, partly from HIPPARCOS parallax data. The largest mass loss rate derived is that for W Aql with (0.8-2.0) $\times 10^{-5}$ M$_\odot$ yr^{-1}, and the lowest is that for *o* Ori with $< 1.2 \times 10^{-9}$ M$_\odot$ yr^{-1}. The S-stars without Tc have smaller mass loss rates, than those with Tc.

Diagrams showing mass loss rate, dust-to-gas ratio and expansion velocity versus pulsation period are presented, and compared to similar data for carbon- and oxygen-rich Miras. The S-Miras stand not out in any way from the C- or O-Miras in these diagrams. In the diagram with expansion velocity versus pulsation period, the S-SRs span the same range in velocity as the S-Miras, but they have periods which are about a factor of 2.5 shorter. This was previously noted for O-rich SRs. As in that case, the most straightforward explanantion is that the SRs among the S-stars pulsate in a higher order pulsation mode.

Key words: circumstellar matter – stars: mass loss – stars: AGB – radio lines: stars

1. Introduction

An important aspect of stellar evolution on the AGB is the process of mass loss. Both the temporal behaviour of the mass loss rate (e.g. Willems & de Jong 1988, Zijlstra et al. 1992, Olofsson et al. 1998) and the time-averaged mass loss rate are of interest. The processes of core growth near the center of an AGB star and the loss of mass in the outer parts determine how long a star can remain on the AGB. Observationally, the mass loss rate can be determined from the infrared properties or from its molecular emission lines. With respect to the first method, one can use an emperical formula, like that of Jura (1987), linking the mass loss rate to the observed infrared flux at 25 or 60 μm. Jura (1988) has applied this method to a sample of S-stars and finds mass loss rates between 1×10^{-8} M$_\odot$ yr^{-1} and 6×10^{-6} M$_\odot$ yr^{-1} with a median around 5×10^{-8} M$_\odot$ yr^{-1}. He derives a dust-to-gas ratio of about 2.0×10^{-3}.

The modelling of the molecular emission around AGB stars is not straightforward, although progress has been made in recent years (e.g. Sahai 1990, Kastner 1992, Justtanont et al. 1994, Groenewegen 1994). Such modelling has not yet been applied to S-stars, and will not be attempted here. Alternatively, one can use the simple formula of Knapp & Morris (1985, also see van der Veen & Oloffson 1990) to estimate the mass loss rate. This formula is based on the kinetic temperature structure of IRC +10 216 and old photodissociation radii for CO. Recently, Kastner (1992) has presented an improved simple formula based on calculations which include the photodissociation radii from Mamon et al. (1988) and a self-consistent gas temperature calculation using an approximate treatment for the heating and cooling terms.

In the literature their exist many CO observations of M- and C-stars. The catalog of Loup (1993) contains entries for about 180 M-stars, about 200 entries for C-stars, but only 11 entries for MS- and S-stars. Because the ratio of the observed number of S-stars to C-stars is about 1/3, it is clear that S-stars have not got the attention in CO observations they arguably deserve. To remedy this, we observed a sample of S-stars with the IRAM telescope in the CO(1-0) and CO(2-1) lines. Bieging & Latter (1994; hereafter BL), Sahai & Liechti (1995; hereafter SL) and Jorissen & Knapp (1998; hereafter JK) also present CO, HCN and SiO observations of MS/S-stars, which partly overlap with ours.

This paper is organised as follows. In Sect. 2 the sample is described. The observations and the results are outlined in Sect. 3. In Sect. 4 a compilation of all MS/S-stars with CO observations is presented and mass loss rates based on the IRAS 60 μm flux and CO observations are calculated. The results are discussed in Sect. 5. Conclusions are presented in Sect. 6.

Send offprint requests to: Martin Groenewegen, (groen@mpa-garching.mpg.de)

⋆ Based on data from the ESA HIPPARCOS astrometry satellite.

Table 1. The observed S-stars

S	identification	R.A. (1950)	Dec. (1950)	Ref.[1]	accuracy	l	b	sp. type	Tc[2]	S_{12} (Jy)	S_{25} (Jy)	S_{60} (Jy)
8	T Cet	00 19 14.5	–20 20 06	SAO	1”	77.5	–80.2	M5-6Se	Y	198.	55.8	14.4
79	BD Cam	03 37 47.7	63 03 25	SAO	1”	140.8	6.4	S4/2	N	41.0	10.8	1.6
103	T Cam	04 35 14.0	66 02 56	S	2”	143.3	12.8	S6/5e	Y	41.3	11.9	3.6
114	*o* Ori	04 49 42.0	14 10 08	SAO	1”	185.4	–18.4	M3S	Y	85.4	21.4	4.6
149	NO Aur	05 37 26.9	31 53 43	SAO	1”	176.9	0.7	M2S	Y, N	43.5	22.9	5.1
931	ST Sco	16 33 24.6	–31 08 01	S	2”	349.3	10.7	S8/4	Y/IR	51.8	21.9	4.5
A[3]	IRC –10 401	18 07 38.5	–10 34 58	Ste	2”	18.8	4.2	S	Y/IR	177.	110.	18.1
1112	S Lyr	19 11 08.4	25 55 16	S	10”	58.6	7.1	SC	Y/IR	42.1	20.2	5.4
1117	T Sgr	19 13 21.3	–17 03 33	S	5”	20.3	–13.0	S5/6	Y	40.3	14.3	4.0
1146	AFGL 2425	19 36 08.7	–16 58 50	G	8”	22.8	–17.9	S	Y/IR	97.8	76.4	10.2
B[4]	-	19 37 07.7	28 55 33	Ste	2”	63.9	3.5	S	Y/IR	50.4	39.1	6.0
1308	RX Lac	22 47 40.6	40 47 08	S	10”	99.5	–16.5	S7.5/1	Y/IR	98.7	32.7	8.4
1322	GZ Peg	23 06 59.6	8 24 21	SAO	1”	84.8	–46.5	M4S	N	80.9	20.1	3.3
1345	WY Cas	23 55 28.9	56 12 32	S	2”	115.6	–5.6	S6/6	Y/IR	50.9	28.4	8.7

Notes. (1) Source of the coordinates: SAO = SAO catalog, S = S-star catalog, PSC = IRAS Point Source Catalog, G = Grasdalen et al. (1983), Ste = Stephenson (1990). (2) The presence or absence of Tc is indicated by a Y (yes) or N (no) (Little et al. 1987, Smith & Lambert 1988). For stars which have not been observed for the presence of Tc we used the infrared criteria of Groenewegen (1993a). All cases are consistent with the presence of Tc, and are labelled Y/IR (yes, on the basis of infrared properties). (3) Listed as number 25 in Stephenson (1990). (4) Listed as number 41 in Stephenson (1990).

2. The sample

Infrared-bright MS and S-stars (we will refer to both categories simply as S-stars) were found by cross-correlating the 1347 stars in the S-star catalog of Stephenson (1984) and the 75 S-stars listed in Stephenson (1990) with the IRAS Point Source Catalog and retaining only those stars with $S_{12} > 40$ Jy. This results in 43 stars. From this list we observed 14 stars. In the literature CO observations are reported by Loup et al. (1993) for 11 objects (10 have $S_{12} > 40$ Jy, none is in our sample), by Bieging & Latter (1994) for 27 objects (13 have $S_{12} > 40$ Jy, 4 are in our sample), by Sahai & Liechti (1995) for 48 objects (20 have $S_{12} > 40$ Jy, 10 are in our sample) and by JK for 12 objects (2 have $S_{12} > 40$ Jy, one is in our sample). Table 1 lists information on the stars observed in the present program: identification, observed position with reference and quoted accuracy of the coordinates, galactic coordinates, spectral type (from the S-star catalog) and IRAS fluxes. Since the observations in 1991, the HIPPARCOS database has become available and we checked for improved coordinates. Six stars are in the HIPPARCOS database. The largest differences are for T Sgr, which is located approximately 6″ south of the observed position, and GZ Peg which is about 0.4^s east of the observed position. In the other cases the differences are less than 2″. T Sgr was detected in the smaller beam at 230 GHz, but its intensity may be underestimated. GZ Peg was not detected and should be reobserved at the improved position. We also list in Table 1 if a star has Technetium in its spectrum or not (data taken from Little et al. 1987, Smith & Lambert 1988 and Jorissen et al. 1993). The data on NO Aur is contradictory. If a star was not observed for the presence of Tc, we used the infrared criteria of Groenewegen (1993a) to infer its status. If the infrared properties of a star are consistent with those of Tc containing stars it is labelled as “Y/IR” in Tab. 1.

3. The observations

The observations were obtained with the IRAM telescope at Pico Vuelta, Spain, between 7-10 August, 1991 in a program to observe carbon stars (see Groenewegen et al. 1996) and S-stars. We used two SIS receivers with two 512 × 1 MHz filterbanks as backend. The ^{12}CO(1-0) and ^{12}CO(2-1) transition were observed simultaneously. For two stars we observed the ^{13}CO(1-0) and ^{13}CO(2-1) transition simultaneously. We used the wobbling secondary with a throw of 120″. The beamwidth and main beam efficiencies are 21″, 0.60 and 12.5″, 0.45 for the J = 1-0 and 2-1 transition, respectively. Linear baselines were removed and the observed line intensities were calibrated using sources in the list of Mauersberger et al. (1989). We estimate the calibration to be accurate to 10 % (1σ).

All temperatures are expressed on a main-beam temperature scale. The J = 2-1 data was smoothed to give a uniform velocity resolution of $\sim$2.6 km s^{-1} for both transitions. The results of the observations are listed in Table 2 were we give the name of the object, the transition, the rms noise, the main-beam peak temperature, the integrated intensity, the central velocity and half the velocity width at zero intensity which equals the expansion velocity of the circumstellar shell. The calibrated profiles are shown in Figs. 1-3.

3.1. Comparison with other observations

Four stars in our sample have been observed by Bieging & Latter (1994) with the NRAO 12m telescope, which has a beam size approximately twice that of IRAM. BL did not detect BD Cam, nor did we. Both BL and we detected ST Sco. BL did not detect T Cam, we did. Scaling our peak intensity down by a factor of 4, which is the square of the ratio of the beam sizes, we estimate an peak intensity of 0.14 K in the NRAO beam at 230 GHz, which

Table 2. Results from the observations

name	transition[(1)]	rms (K)	$T_{\rm peak}$ (K)	$\int T$ dv (K km/s)	v_c (km/s)	v_∞ (km/s)
T Cet	1-0	0.044	0.14	1.3		
	2-1	0.077	0.5	≈ 6.2	≈ 22	≈ 10
BD Cam	1-0	0.030				
	2-1	0.10				
T Cam	1-0	0.021	0.18	1.6 ± 0.1	-12.2 ± 0.2	5.8 ± 0.3
	2-1	0.096	0.55	4.1 ± 0.3	-11.6 ± 0.7	7.0 ± 0.2
o Ori	1-0	0.027				
	2-1	0.086				
NO Aur	1-0	0.031				
	2-1	0.072				
ST Sco	1-0	0.063	0.3	≈ 3.3	≈ -4	≈ 10
	2-1	0.15	0.6	≈ 8.0	≈ -4	≈ 10
S A	1-0	0.036	0.12	2.9 ± 0.3	21.9 ± 0.7	16.7 ± 0.9
	2-1	0.068		≈ 4.1		
S Lyr	1-0	0.027	0.15	3.1 ± 0.2	50.3 ± 1.0	14.0 ± 1.1
	2-1	0.060				
T Sgr	1-0	0.027				
	2-1	0.058	0.30	≈ 3.4	≈ 8	≈ 10
AFGL 2425	1-0	0.036	0.18	2.4 ± 0.3	55.9 ± 0.8	11.9 ± 0.9
	2-1	0.072	0.40	4.8 ± 0.6	57.8 ± 0.9	11.9 ± 1.0
S B	1-0	0.029	0.05	≈ 1.9[(2)]	≈ 20	≈ 20
	2-1	0.072	0.10	≈ 3.3[(2)]	≈ 20	≈ 20
RX Lac	1-0	0.021	0.30	2.0 ± 0.3	-15.4 ± 0.1	6.5 ± 1.0
	2-1	0.055	1.2	6.9 ± 0.2	-15.7 ± 0.1	4.8 ± 1.0
	^{13}CO(1-0)	0.022		<0.7		
	^{13}CO(2-1)	0.037	0.08	≈ 0.8		
GZ Peg	1-0	0.028				
	2-1	0.077				
WY Cas	1-0	0.036	0.25	6.4 ± 0.2	7.7 ± 0.2	13.5 ± 0.3
	2-1	0.062	1.1	23.2 ± 0.3	8.2 ± 0.2	17.5 ± 0.5
	^{13}CO(1-0)	0.021		<2.0		
	^{13}CO(2-1)	0.039		<3.8		

Notes. (1) Unless otherwise indicated the ^{12}CO transition is listed. (2) The interstellar feature at v = 21 km/s was removed to calculate the integrated intensity.

is at the 3 σ level of their observations. BL did not detect T Sgr, we detected the J = 2-1 line. Scaling again our peak intensity to the NRAO 230 GHz beam, we predict an intensity of 0.075 K, which is at 1.8σ level of their observations. Both non-detections by Bieging & Latter can be accounted for by the expected lower peak temperature in the larger NRAO beam.

Ten stars in our sample have been observed by Sahai & Liechti (1995) with IRAM and SEST. BD Cam, *o* Ori, NO Aur and GZ Peg are not detected by SL, nor by us. ST Sco, T Sgr, RX Lac and WY Cas are detected by SL and by us. The two sources were discrepancies arise are T Cam and S Lyr. T Cam is not detected by SL using IRAM, but is by us. SL even have a lower rms noise in their spectra and should have detected it at the 10σ level. Variability could be an explanation, but variability at this level is unheard of. Possibly they pointed at the incorrect (IRAS) position; their position differs by 11″ from ours. This is almost one beamsize at 230 GHz and could explain part of this discrepancy. The other object is S Lyr, which SL detect in the J = 2-1 line at a level which corresponds to 6σ in our spectrum. We are at a loss to explain this discrepancy as both SL and we pointed to the same position within 1.5″. NO Aur is observed by us and JK. Neither group detected the source.

The stellar velocities based on optical or other data agree with the CO measurements, when available. This is the case for the optical velocities for T Cet, RX Lac and T Sgr, and the velocity derived from water maser observations for S B (Engels & Lewis 1996).

4. Mass loss in S-stars

In this section we will derive the mass loss rate in the gas and dust. Table 3 compiles all S-stars with CO J = 1-0, and/or J = 2-1 observations. Two stars recently observed (but not detected) only in the J = 3-2 transition (by JK) are not included as the method that will be used to derive the gas mass loss rates is only valid for J = 1-0 and 2-1 observations. Also the following restrictions apply: When both detection(s) and upperlimits exist for lines of a given star, only the reference to the detection(s) are given and used to derive the gas mass loss rate per unit

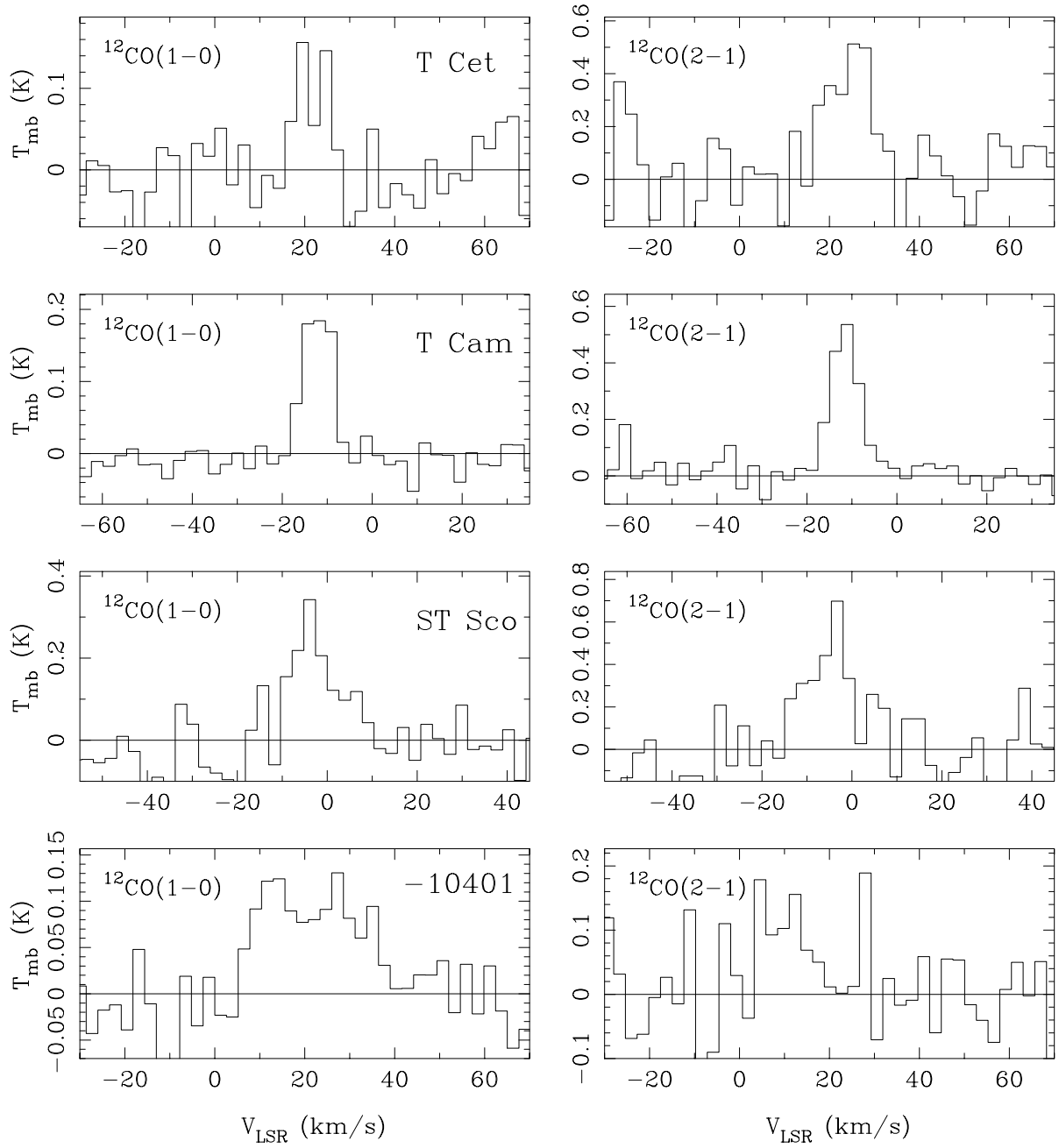

Fig. 1. CO observations. Lefthand panel J = 1-0, righthand panel J = 2-1 transition.

distance; peak temperatures detected at a level lower than 3σ are not included; references where the integrated intensity but not the peak temperature are given, are also not included.

Listed in Table 3 are the number in the S-star catalog (Stephenson 1984), the name or identifier, whether the star is an intrinsic or extrinsic S-star (see below), the 60 μm flux, variability type and period, and the reference to the CO observations. From Sahai & Liechti the stars TV Dra and RZ Peg are not considered. Of the former, Stephenson (1984) explicitly states that it is not an S-star but an M-star, and the latter object is a C-star. The intrinsic or extrinsic character is inferred from the direct observation of Technetium (from Groenewegen 1993a, Jorissen et al. 1993), or indirectly from the infrared properties (see Groenewegen 1993a, Jorissen et al. 1993).

Table 3 contains 15 stars that are not in the similar CO compilation of S-stars of JK. For three of those the first ever observation is reported in the present work. Two of them have not been observed by IRAS, which was one of the selection criteria by JK, and two of them have an upperlimit at 60 μm while JK required a detection at this wavelength. Four of them are for some reason not in their fundamental list of IRAS detected S-stars (their Table 1), although these are S-stars and have good quality

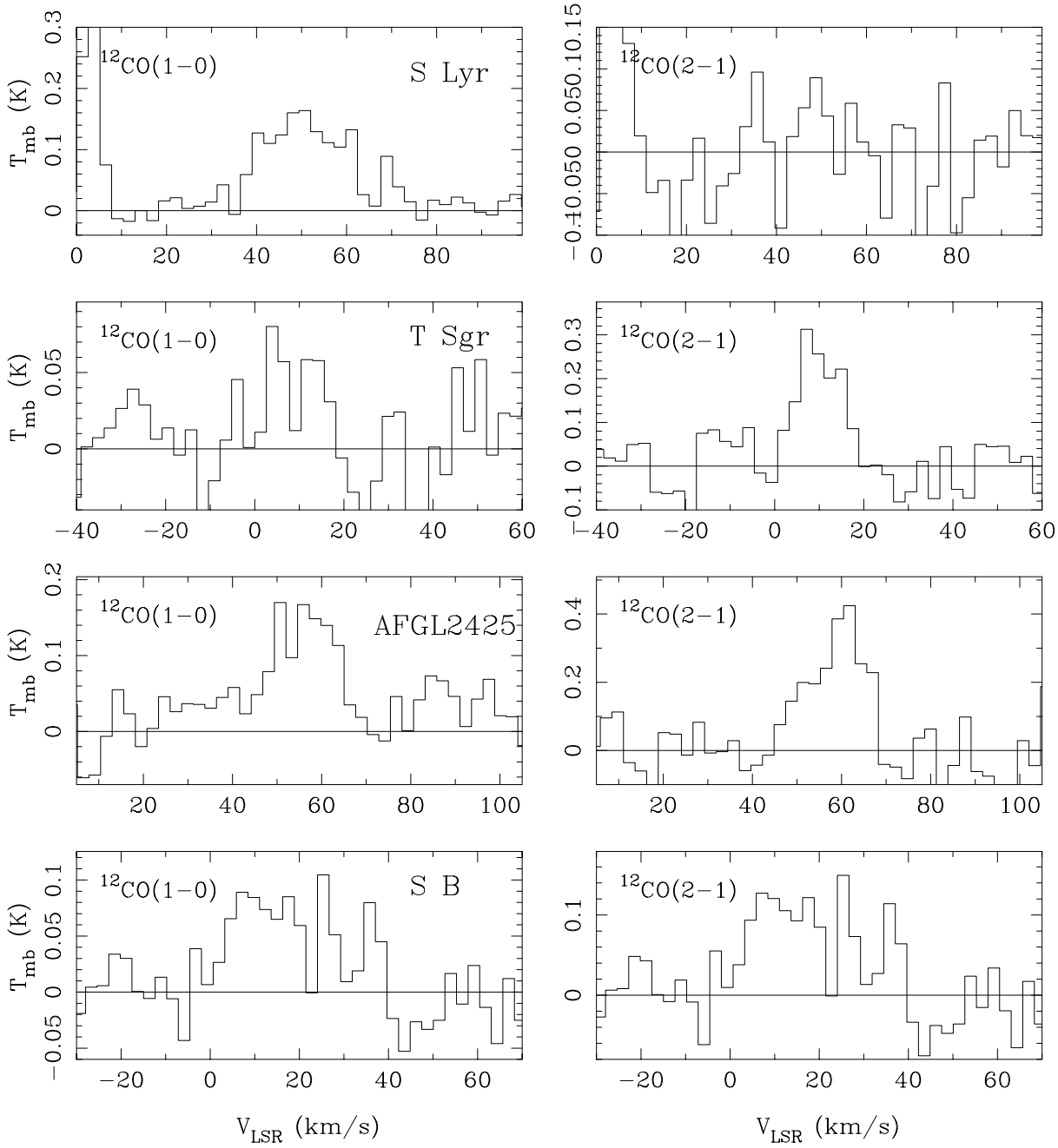

Fig. 2. CO observations. As Fig. 1.

IRAS fluxes at 12, 25 and 60 μm. Finally, the remaining three are in their fundamental list, but the existing CO data seems to have been overlooked. Conversely, their list of CO observations (their Table 6) includes 4 stars that are not in our Table 3. These are TV Dra and RZ Peg, for reasons explained above, and the two stars detected only in the J = 3-2 line.

4.1. CO Detection statistics

Of the 6 stars without Tc, and *o* Ori, the star with a white dwarf companion, only one star (DY Gem) is detected in CO. However this star has all characteristics of a true AGB star (see Groenewegen 1993a). The sample is small but the result supports the finding from the infrared properties that these stars have no or very little CS material (see Groenewegen 1993a). These stars are probably not on the AGB but acquired their s-process material at the time when the present-day white dwarf was on the AGB.

The brightest star with Tc, not detected in CO, has a 60 μm flux of 3.6 Jy. Above that value, all stars with Tc are detected in CO. The detection statistics are summarised in Table 4. This tabulation may be usefull in planning further survey type observations.

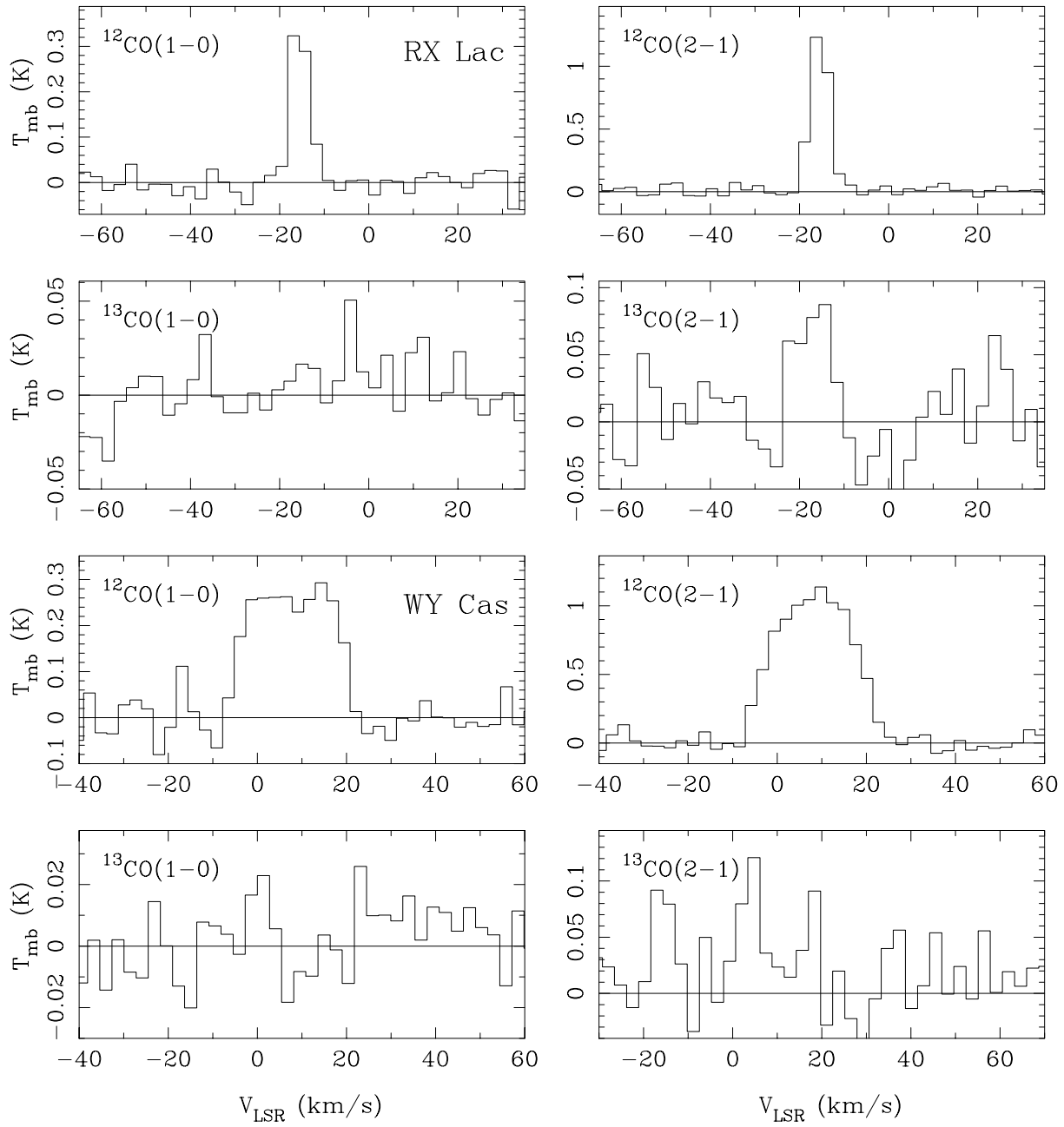

Fig. 3. CO observations of the two stars for which ^{12}CO and ^{13}CO was obtained.

4.2. Mass loss from CO

There is a relation between the measured peak intensity of a CO line and the mass loss rate. From Olofsson et al. (1993) we use:

$$\dot{M}_{\rm g} = 1.4 \times \frac{T_{\rm mb}\, v_\infty^2\, D^2\, B^2}{2 \times 10^{19}\, f_{\rm CO}^{0.85}\, s(J)} \qquad (1)$$

where $\dot{M}_{\rm g}$ is in solar masses per year, $T_{\rm mb}$ in Kelvin, v_∞ in km s^{-1}, D the distance in parsec, B the FWHM size of the telescope beam in arcsec, $f_{\rm CO}$ the CO abundance relative to H_2, and $s(J)$ is a correction factor, equal to unity for the J = 1-0 transition and 0.6 for the J = 2-1 transition.

This relation was used with $f_{\rm CO} = 5 \times 10^{-4}$ to calculate the mass loss rate per unit distance. The results are listed in Table 5. When multiple CO measurements exist (see the reference list in Table 4), the range in the mass loss rate is indicated. For FU Mon, JK convincingly argue that the results obtained by Sahai & Liechti are in error. Therefore only the JK data is used to estimate the gas mass loss rate. The expansion velocity listed is an appropriate average over the available data. Three sigma upper limits are also listed, using an assumed expansion velocity of 5 km s^{-1} (values between parenthesis).

Table 3. S-stars with CO observations

S	Ident.	Tc[1]	S_{12} (Jy)	S_{25} (Jy)	S_{60} (Jy)	Var. type	Period (days)	Ref. CO
8	T Cet	Y	198.	55.8	14.4	SRb	159	1
9	R And	Y	327.	168.	24.2	M	409	2, 7
20	V365 Cas	Y/IR	21.1	7.77	2.40	SRb	136	2, 3
28	S Cas	Y/IR	342.	195.	26.8	M	612	2, 8
49	W And	Y	167.	72.1	13.4	M	396	2, 5
79	BD Cam	N	41.0	10.8	1.59	Lb		1,2,3
89	HD 26816	Y	24.4	7.30	2.63	Lb:		13
103	T Cam	Y	41.3	11.9	3.63	M	373	1
114	o Ori	Y	85.4	21.4	4.57	SRb	30:	1
116	TV Aur	Y/IR	12.9	4.25	1.26	SRb	182	2
133	HD 35155	N	7.98	2.02	0.41			3
149	NO Aur	Y, N	43.5	22.9	5.12	Lc		1, 13
212	FU Mon	?	17.0	4.73	1.65	SR	310	3, 13
231	DY Gem	N	21.7	10.4	2.59	SRa	1145	3
283	R Lyn	Y/IR	18.0	5.66	1.34	M	379	2, 13
307	R Gem	Y	21.6	7.52	2.34	M	370	3, 4
312	AA Cam	Y	14.5	6.07	1.86	Lb		3
326	RR Mon	Y/IR	26.8	11.6	2.00	M	395	3
347	Y Lyn	Y	122.	64.2	11.4	SRc	110	9
387	SU Mon	Y/IR	19.4	7.08	2.01	Lb		3
542		Y/IR	14.6	6.53	2.74			3
589	RS Cnc	Y	48.0	20.9	32.6	SRc:	120:	5, 13
614	UU Vel	Y/IR	11.6	5.92	$<$1.90	M	409	3
626	FM Hya	Y/IR	9.71	4.02	0.74	M	300	13
704	Z Ant	Y/IR	30.5	14.2	1.92	SR	104	13
796	HR 4755	N/IR	18.2	4.11	0.65			13
803	S UMa	Y	4.23	1.40	0.29:	M	226	13
816	UY Cen	Y/IR	54.8	20.5	4.13	SR	115:	3
817	TT Cen	Y/IR	21.1	12.3	7.15	M	462	3
826	HD 118685	N/IR	23.5	6.34	1.12			3
830	AM Cen	Y/IR	15.6	5.52	2.06	Lb		3
834	VX Cen	Y/IR	46.4	14.2	3.56	SR	308	3
872	GI Lup	Y/IR	21.8	8.94	2.10	M	326	3
903	ST Her	Y	199.	97.1	16.7	SRb	148	3, 10
927		Y/IR	9.80	4.97	0.91			3
931	ST Sco	Y/IR	51.8	21.9	4.49	SRa	195	1, 2, 3
954	RT Sco	Y/IR	161.	67.0	18.8	M	449	3
962		Y/IR	85.0	68.4	13.9			3
978	V521 Oph	Y/IR	38.2	11.7	2.67	SRb	320	2, 3
1003	KW Sgr	Y/IR	250.	148.	18.4	SRc	670	3
1004	V407 Sco	?	-	-	-	M	396	3
A[2]	IRC-10401	Y/IR	177.	110.	18.1			1
1093	VX Aql	Y/IR	16.1	5.61	1.72	M:		3
1096	ST Sgr	Y/IR	52.3	19.4	4.15	M	395	2, 3
1112	S Lyr	Y/IR	42.1	20.2	5.41	M	296	1, 3
1115	W Aql	Y/IR	1575.	670.	112.	M	490	2, 3, 4
1117	T Sgr	Y	40.3	14.3	4.04	M	395	1, 3
1141	EP Vul	Y/IR	31.6	13.8	3.01	Lb		2, 3
1146	AFGL 2425	Y/IR	97.8	76.4	10.2			1
1150	R Cyg	Y	105.	52.2	11.9	M	426	2, 11
B[3]	-	Y/IR	50.4	39.1	6.01			1
1165	χ Cyg	Y	1690.	459.	80.7	M	408	2, 3, 12
1188	AA Cyg	Y	39.7	15.5	5.27	SRb	213	3
1189	DK Vul	Y/IR	18.6	8.23	3.84	SRa	370	2, 3
1195	HD 191630	Y	10.6	2.90	1.12			3
1196	RZ Sgr	Y/IR	38.2	25.0	10.1	SRb	223	3
1219	V441 Cyg	?	12.8	3.95	$<$11.5	SRa	375	2
1224	AD Cyg	?	10.3	3.04	$<$0.7	Lb		2
	CY Cyg	?	-	-	-	Lb		3
1294	π Gru	Y	909.	437.	77.3	SRb	150:	3, 5, 6
1308	RX Lac	Y/IR	98.7	32.7	8.39	SRb	650:	1, 3
1314	DB 42141	Y/IR	109.	93.3	16.7			3
1315	HR Peg	Y	27.6	7.15	1.19	SRb	50:	2
1322	GZ Peg	N	80.9	20.1	3.30	SRa	93	1, 3
1345	WY Cas	Y/IR	50.9	28.4	8.69	M	477	1, 3
1346	W Cet	Y	13.3	3.96	0.73	M	351	2, 3

Notes. References for the CO data: 1 = this paper, 2 = Bieging & Latter (1994), 3 = Sahai & Liechti (1995), 4 = Heske (1990), 5 = Nyman et al. (1992), 6 = Sahai (1992), 7 = Bujarrabal et al. (1986), 8 = Heske (1989), 9 = Wannier & Sahai (1986), 10 = Margulis et al. (1990), 11 = Zuckerman et al. (1986), 12 = Bujarrabal & Alcolea (1991), 13 = Jorissen & Knapp (1998).
[1] Indicates the presence of Tc. When no spectral information is available, we use the infrared criteria of Groenewegen (1993). All cases consistent with the presence of Tc are labelled Y/IR (yes, on the basis of infrared properties), the others as N/IR
[2] Listed as number 25 in Stephenson (1990).
[3] Listed as number 41 in Stephenson (1990).

Table 4. CO detection statistics for stars with Tc

S_{60} (Jy)	CO yes	CO no
<1	0	4
1–3	10	7
3–9	13	2
9–27	14	0
27–81	3	0
81–243	1	0

4.3. Mass loss from dust

There is a relation between the 60 (or 25) μm flux and the dust mass loss rate. From Jura (1988) we have:

$$\dot{M}_{\rm d} = C\, v_{15}\, D^2\, L_4^{-0.5} \lambda_{10}^{0.5}\, \kappa_{150}^{-1}\, F(\lambda) \quad (2)$$

where $\dot{M}_{\rm d}$ is in solar masses per year, C is a constant, v_{15} is the dust expansion velocity in units of 15 km s^{-1}, D the distance in kpc, L_4 the luminosity in units of 10 000 L$_\odot$, λ_{10} the wavelength in units of 10 μm where the peak of the energy distribution occurs, and κ_{150} the opacity at 60 μm in units of 150 cm^{2}g^{-1}. $F(\lambda)$ is the excess emission at wavelength λ in Jansky. Jura (1988) uses C = 7.7 $\times$ 10^{-10} and λ = 60 μm.

It is clear that the *excess* emission should be used in Eq. 2, but in many application of this formula, the *observed* flux is used (e.g. Whitelock et al. 1994, Guglielmo et al. 1993, Jura & Kleinmann 1992, Epchtein et al. 1990, Jura 1988, Claussen et al. 1987). This can lead to a severe overestimate of the mass loss rate when the stellar contribution to the observed flux is large, that is for small mass loss rates. To make a first order correction for this effect some radiative transfer models were calculated using the code of Groenewegen (1993b). A dust shell composed of silicate grains (from Volk & Kwok 1988) was placed around a M5 central star (model atmosphere from Fluks et al. 1994). The inner dust temperature was set at 1000 K. Shells of increasing optical depth were calculated and the fraction of excess emission determined as a function of S_{12}/S_{25} ratio. The result is displayed in Fig. 4. It shows that for this particular model, neglect of the stellar contribution to the observed 60 μm flux leads to an overestimate of the dust mass loss rate by factors larger than two, for flux ratios $S_{12}/S_{25} > 3$. From the same modelling we determined the constant C, which is used in this paper: C = 1.34 $\times$ 10^{-9} for λ = 60 μm, and C = 7.67 $\times$ 10^{-11} for λ = 25 μm. The factor of two difference in the value for C at 60 μm compared to Jura indicates the intrinsic uncertainty of this method. Kerschbaum et al. (1996) made a similar approach and also estimated the contribution to the observed 60 μm flux by the stellar photosphere.

Using Eq. 2, the dust mass loss rates are determined with the above mentioned values for C, and an opacity κ_{150} = 1.0. λ_{10} is taken to be 0.11, which also follows from our radiative transfer modelling, almost independent of the mass loss rates considered here. The dust velocity is assumed equal to the gas velocity, which implies that the drift velocity is neglected. The drift velocity depends on the uncertain effective grain efficiency factor, usually denoted Q. As the drift velocity may become comparable in size to the gas velocity, it implies that the dust mass loss rates quoted below may be systematically too low by up to a factor of 2. The derivation of the luminosity and distance is discussed below. Two stars have not been observed by IRAS and hence no dust mass loss rate could be derived. The dust mass loss rates per unit distance are listed in Table 5. The gas-to-dust mass ratio is also listed. For the gas mass loss rate the geometric mean of the available values is taken.

4.4. Distance and luminosity

To calculate the dust mass loss rate, knowledge of the luminosity is required (see Eq. 2). Although the gas-to-dust ratio is independent of distance, the absolute values of both the gas

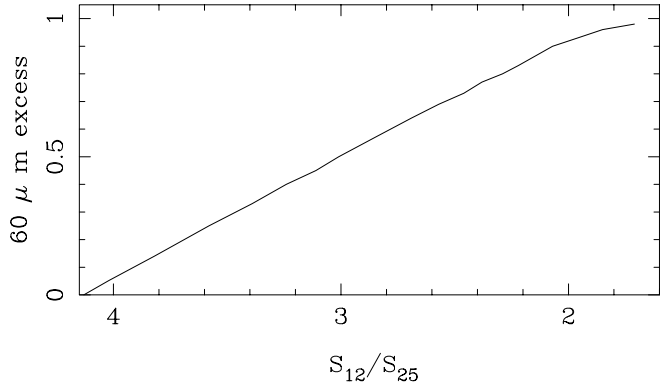

Fig. 4. Fraction of excess emission at 60 μm, as a function of flux-ratio at 12 and 25 μm, for the model described in the Sect 4.3.

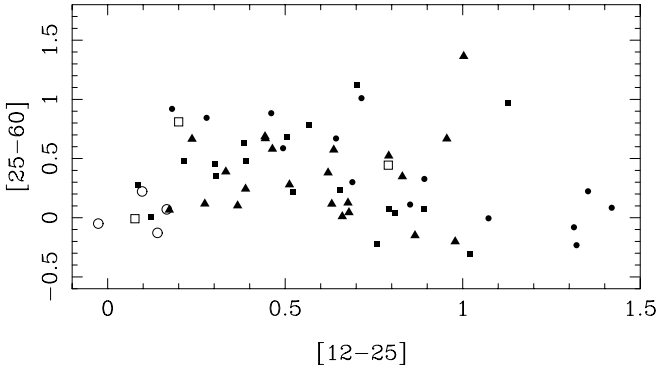

Fig. 5. IRAS colour-colour diagram for the S-stars with CO observations. Symbols: fileed box = SR with Tc, □ = SR without or unknown Tc, filled triangle = Mira with Tc, △ = Mira without or unknown Tc, • = other stars with Tc, ○ = other stars without Tc.

and dust mass loss rate also require knowledge of the distance. Distance and luminosity are calculated as follows.

Groenewegen et al. (1997) presented first results for late-type stars based on a sub-set of HIPPARCOS data, made available to us in the fall of 1996. The sample included 16 MS- and S-stars. Three stars with an Hipparcos parallax are in the present sample. For these three stars the luminosities are directly taken from Groenewegen et al. (1997) who modelled the SEDs.

Since then, the entire HIPPARCOS catalog became available, and all stars in the sample were checked for a parallax. Table 5 includes those parallaxes that are non-negative and with an accuracy of better than 50%. In addition, apparent K-magnitudes were taken from the IRC catalog, when available, or otherwise from the Gezari et al. (1993) compilation or other recent literature data. In the latter cases no attempt to transform these magnitudes to the IRC system is attempted. A discussion on HIPPARCOS data for S-stars in general can be found in Van Eck et al. (1998).

For stars with a parallax, the absolute K-magnitude follows from the observed distance and the apparent K-magnitude. This treatment neglects the influence of the Lutz-Kelker bias (Lutz & Kelker 1973), the importance of which was recently discussed in the connection with Cepheids (Oudmaijer et al. 1998). Neglect of this bias, depending on the exact assumptions and treatment, in many cases leads to an underestimate of the luminosity. On the other hand, the luminosity enters only through the square root in Eq. (2), and therefor the errors due to the neglect of the Lutz-Kelker bias are expected to be much smaller than the uncertainties due to the method (that is, the uncertainty in C), and the drift velocity. The absolute bolometric magnitude (and luminosity) are calculated assuming a bolometric correction at K of 3.0, which is appropriate for stars with the relatively low mass loss rates discussed here (Wood et al. 1983, Groenewegen 1997).

For the Miras in the sample (and without parallax), the relation between absolute K-magnitude and pulsation period for oxygen-rich Miras is used (Feast et al. 1989) to derive $M_{\rm K}$. The luminosity is derived in the way described above, and the distance is estimated from the absolute and apparent K-magnitude. For the SR and irregular variables (without parallax) we proceeded as follows. For the stars in Groenewegen et al. (1997) we have calculated the absolute K-magnitudes and luminosities for the non-Mira S-stars which definitely are intrinsic, or extrinsic, S-stars, respectively. From 5 intrinsic S-stars we derive $M_{\rm K} = -7.1$ and L = 3300 L$_\odot$, from 5 extrinsic S-stars we find $M_{\rm K} = -5.5$ and L = 850 L$_\odot$ (Groenewegen et al. 1997). Formally, these K values refer to the system defined by the IRC catalog. These luminosities and K-magnitudes are adopted for the stars in the sample. For o Ori which has Tc but is unlikely to be on the AGB we adopt the value for the extrinsic S-stars. For DY Gem for which no Tc has been detected, but almost certainly is a intrinsic S-star we take the corresponding absolute K-magnitude (both cases are discussed in detail in Groenewegen 1993a). For the stars for which the intrinsic or extrinsic character could not be derived intermediate values of $M_{\rm K} = -6.3$ and L = 1610 L$_\odot$ are adopted. Four stars in the sample have no K-band observations and no estimate for the distance is listed in Table 5.

No correction for interstellar extinction is made for any of the stars. Most stars are within 1 kpc, and interstellar extinction corrections are generally smaller than the error in the adopted absolute K-band magnitudes, or the uncertainty in the apparent magnitudes, due to variability.

5. Discussion

Fig. 5 shows the IRAS colour-colour diagram of the S-stars with CO data (Table 3). A more complete discussion on various colour-colour diagrams of IRAS detected S-stars with good quality fluxes is given in JK. An IRAS colour-colour diagram with all S-stars which have been searched for Technetium is shown in Groenewegen (1993a). Fig. 5 confirms that result, in the sense that S-stars without Tc have a small IRAS excess. The exception is DY Gem at $[12-25] = 0.79$, but as discussed before this stars has all the characteristics of an intrinsic S-star.

Fig. 6 shows the relation between mass loss rate and pulsation period. The median mass loss rates per unit distance and the derived distances in Table 5 are used to calculate the total

Table 5. Mass loss rates

S	identification	$M_{\rm K}$ (mag.)	L ($L_\odot$)	parallax (mas)	D (pc)	v_∞ (km s^{-1})	$\dot{M}_{\rm g}/D^2$ (10^{-7} M$_\odot$/yr/kpc^2)	$\dot{M}_{\rm d}/D^2$ (10^{-10} M$_\odot$/yr/kpc^2)	gas-to-dust ratio
8	T Cet	−7.6	5540	4.21 ± 0.85	240	10.	2.8-5.8	14.1	285
9	R And	−8.1	8090		480	9.0	17.6-39.9	66.8	400
20	V365 Cas	−7.1	3300		500	7.2	0.42	5.4	79
28	S Cas	−8.7	14190		1110	22.0	65.4-93.0	147.	525
49	W And	−8.0	7730		600	9.0	11.0-31.6	31.7	490
79	BD Cam	−5.8	1000	6.27 ± 0.63	160	(5)	<0.45	(1.1)	<400
89	HD 26816	−6.2	1410	3.79 ± 1.05	260	(5)	<0.34	(3.6)	<95
103	T Cam	−7.9	7110		480	6.4	1.5-2.6	2.4	810
114	o Ori	−6.6	2200	6.02 ± 0.94	170	(5)	<0.40	(0.89)	<450
116	TV Aur	−7.1	3300		490	(5)	<1.0	(0.17)	<5950
133	HD 35155	−5.5	850		330	(5)	<0.75	(0.15)	<5140
149	NO Aur	−7.3	3930	2.38 ± 0.97	420	(5)	<0.17	(11.5)	<15
212	FU Mon	−6.3	1610		380	2.8	0.79	0.85	930
231	DY Gem	−7.1	3300		560	8.0	2.0	9.6	210
283	R Lyn	−7.9	7310		890	8.6	1.4-4.0	1.6	1450
307	R Gem	−7.9	7050		1010	5.0	3.2-4.4	2.4	1600
312	AA Cam	−7.1	3300		560	17.9	2.4	13.2	180
326	RR Mon	−8.0	7730		1100	(5)	<0.20	(2.6)	<75
347	Y Lyn	−7.5	4130	4.03 ± 1.33	248	5.4	5.6	27.2	200
387	SU Mon	−7.1	3300		490	(5)	<0.27	(3.1)	<90
542		−7.1	3300		560	(5)	<1.1	(5.9)	<190
589	RS Cnc	−7.1	3300	8.21 ± 0.98	120	7.2	27.2-36.1	96.8	320
614	UU Vel	−8.1	8090		1230	(5)	<7.5	(0.52)	<14500
626	FM Hya	−7.6	5420		—	(5)	<0.34	(1.1)	<300
704	Z Ant	−7.1	3300		580	7.4	2.6	6.2	420
796	HR 4755	−6.1	1290	3.55 ± 0.76	280	(5)	<0.17	(<0.03)	—
803	S UMa	−7.2	3660		1150	(5)	<0.17	(0.35)	<480
816	UY Cen	−7.1	3300		350	13.1	3.9	17.9	220
817	TT Cen	−8.2	9640		1140	25.4	31.6-61.1	53.7	820
826	HD 118685	−6.3	1970	3.42 ± 0.65	292	(5)	<0.68	(0.66)	<1030
830	AM Cen	−7.1	3300		580	5.4	2.1-2.3	3.3	680
834	VX Cen	−7.1	3300		340	(5)	<2.6	(3.7)	<710
872	GI Lup	−7.7	5920		820	14.0	7.7	8.5	911
903	ST Her	−8.3	9820	3.22 ± 0.75	310	9.1	4.7-7.5	41.2	140
927		−7.1	3300		—	(5)	<0.53	(2.2)	<240
931	ST Sco	−7.1	3300		350	7.5	3.3-7.1	13.4	310
954	RT Sco	−8.2	9200		510	11.0	8.6-21.9	49.1	280
962		−7.1	3300		—	20.	10.2-12.8	143.	80
978	V521 Oph	−7.1	3300		370	(5)	<0.74	(2.8)	<270
1003	KW Sgr	−7.1	3300		480	(5)	–	47.5	–
1004	V407 Sco	−8.0	7730		—	(5)	<0.61	–	–
A	IRC –10 401	−7.1	3300		720	16.7	6.6	156.	42
1093	VX Aql	−7.1	3300		950	7.8	1.2	3.9	300
1096	ST Sgr	−8.0	7730		640	10.0	3.4-5.5	9.0	480
1112	S Lyr	−7.6	5200		1880	14.0	5.8-9.9	28.0	270
1115	W Aql	−8.3	10380		680	19.0	164.-425.	483.	600
1117	T Sgr	−8.0	7730		770	12.0	3.4-5.4	9.7	440
1141	EP Vul	−7.1	3300		410	5.3	1.9-5.8	6.6	490
1146	AFGL 2425	−7.1	3300		830	11.9	5.0-6.6	62.6	92
1150	R Cyg	−8.1	8550		1000	10.2	16.0-18.8	35.4	490
B	-	−7.1	3300		—	20.	4.0-4.7	61.8	67
1165	χ Cyg	−7.5	5140	9.43 ± 1.36	106	8.9	50.0-68.3	59.3	985
1188	AA Cyg	−7.1	3300		350	4.8	2.8	9.0	310
1189	DK Vul	−7.1	3300		580	5.0	1.1-3.2	8.0	260
1195	HD 191630	−7.1	3300		580	(5)	<2.6	(0.58)	<4500
1196	RZ Sgr	−7.1	3300		480	11.4	42.4-50.3	59.4	150
1211	V865 Aql	−7.9	7090		770	(5)	<1.1	(0.64)	<170
1219	V441 Cyg	−6.3	1610		400	(5)	<2.2	(0.33)	<6700
1224	AD Cyg	−6.3	1610		320	2.4	0.38	0.091	4120
	CY Cyg	−6.3	1610		500	(5)	<0.26	–	–
1294	π Gru	−8.0	6920	6.54 ± 1.01	153	15.0	67.3-284.	372.	380
1308	RX Lac	−7.1	3300		240	5.0	1.5-3.5	10.8	200
1314	DB 42141	−7.1	3300		650	19.6	6.8	168.	40
1315	HR Peg	−5.4	710	3.37 ± 0.94	300	(5)	<0.59	(0.66)	<890
1322	GZ Peg	−6.0	1200	4.28 ± 0.88	230	(5)	<0.34	(0.73)	<470
1345	WY Cas	−8.3	10000		1380	15.0	11.1-28.8	37.5	430
1346	W Cet	−7.8	6550		830	(5)	<0.67	(0.47)	<1440

Notes. A velocity of 5 km s^{-1} between parenthesis means an assumed value. For four stars the method to derive the distance from the absolute K-magnitude can not be applied as there is no published apparent magnitude.

mass loss rate. The non-variable stars or those without known period are plotted at constant values of $\log$ P = 1.2 (those with Tc), and 1.3 (those without or unknown Tc content). The Miras in the sample follow reasonably well the relation established over a large period range for C-rich Miras (Groenewegen et al. 1998). The SRs down to periods of 100 days appear to fall on an extension of this relation. The S-stars without Tc have smaller mass loss rates than those with Tc. This is consistent with the conjecture (Groenewegen 1993a, Jorissen et al. 1993, and references therein) that intrinsic S-stars are thermally-pulsing AGB

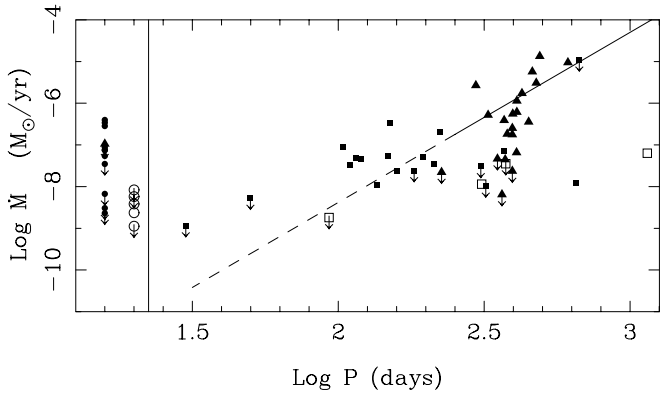

Fig. 6. Mass loss rate versus pulsation period. Symbols as in Fig. 5. The solid line represents the relation for carbon-rich Miras from Groenewegen et al. (1998), and the dashed line is the extension to shorter periods. The shortest period for carbon-rich Miras is about 250 days. S-stars without known pulsation period are plotted at a value of $\log$ P = 1.3 (no or unknown Tc), or 1.2 (with Tc).

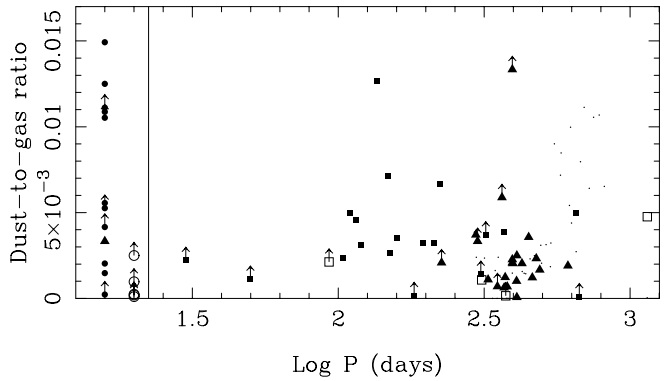

Fig. 7. Dust-to-gas ratio versus pulsation period. Symbols as in Fig. 5. S-stars without known pulsation period are plotted at a value of $\log$ P = 1.3 (no or unknown Tc), or 1.2 (with Tc). Small dots represent the data for the carbon Miras analysed in Groenewegen et al. (1998).

stars, and extrinsic S-stars are not. The largest mass loss rate derived is that for W Aql with (0.8-2.0) $\times$ 10^{-5} $M_\odot$ yr^{-1}, and the smallest mass loss rate found is that for o Ori with $< 1.2 \times 10^{-9}$ $M_\odot$ yr^{-1}.

There exists the possibility that we may have missed a possible narrow line in our observations, since we used a coarse velocity resolution of 1 MHz. In particular since o Ori has a wide dwarf companion, and there are now (at least) two examples known of CO emission from a circumbinary disk where the CO emission lines are narrow (The Red Rectangle [Jura et al. 1995], and BM Gem [Kahane et al. 1998]). To a certain extent this is true, although in both cases the narrow emission line is on top a much broader underlying emission component, which we would have easily detected. Also in the case of the Red Rectangle, the CO integrated emission is very low compared to its 60 μm flux (Jura et al. 1995), compared to that ratio in AGB stars (Olofsson et al. 1993). For o Ori, the ratio of 12 to 25 μm flux of 4.0 already indicates, following Fig. 4, that only about 10% of the 60 μm flux is circumstellar.

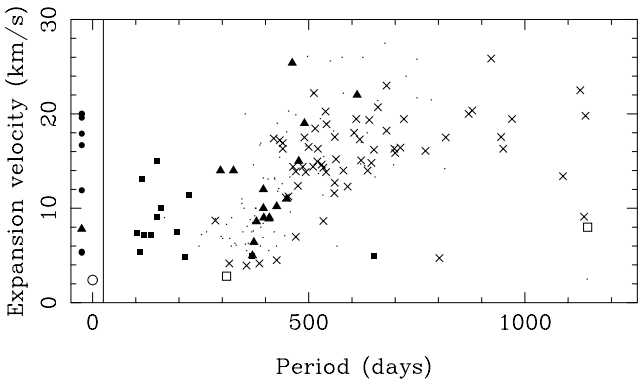

Fig. 8. Expansion velocity versus pulsation period. Symbols as in Fig. 5. S-stars without known pulsation period are plotted at a value of v = 0 (no or unknown Tc), or –25 km s^{-1} (with Tc). The small dots represent the carbon Miras from Groenewegen et al. (1998). The crosses are values for O-rich Miras and OH/IR stars, as compiled by Groenewegen et al. (1998).

Using this corrected flux and the relations shown in Olofsson et al. one would expect an integrated CO emission in the IRAM beam of 0.2-0.5 K km s^{-1}. This is comparable to the derived 3σ upper limits assuming a rectangular profile with a width of 10 km s^{-1}, and so based on these arguments it can not be claimed that the CO/60μm ratio is unusually low which could be interpreted as indicating the presence of a circumbinary disk, or photodissocation of CO by a hot companion. New, very long integrations at an increased velocity resolution may address this possibility further.

Fig. 7 shows the dust-to-gas ratio as a function of pulsation period. The arithmetic mean and median value are both 0.0030, which is slightly larger than the value derived by Jura (1988). The dust-to-gas ratio for the extrinsic S-stars is smaller than for the intrinsic ones. For the S-Miras there is good overlap with carbon Miras of the same period. One might have expected otherwise, since, if the oxygen-abundance is almost equal to the carbon abundance in S-stars, there is little oxygen left that could condense onto grains. Apparently this is not the case, possibly suggesting an effective dust formation, or that our sample does not include S-stars where the C/O ratio is sufficiently close to unity for poor dust formation to occur.

Fig. 8 shows the expansion velocity as a function of period. A similar diagram is shown in JK, but without discussion. Also shown are data for C-rich Miras, O-rich Miras and OH/IR stars (from Groenewegen et al. 1998). The S-Miras follow this sequence almost perfectly. The S-SRs have expansion velocities that span the same range as the bulk of the S-Miras but their periods are shorter by a factor of about 2.5. The same was noticed by Kerschbaum et al. (1996) and Kerschbaum & Olofsson (1998) for oxygen-rich SRa and SRb's. As already noted by them, the most straightforward explanation for this difference between SRs and Miras is to assume that the SRs pulsate in a higher order pulsation mode.

6. Conclusions

^{12}CO J = 1-0 and 2-1 observations of 14 S-stars are presented, and 6 new detections are reported. A compilation is presented of all CO observations for S-stars. The stars in this sample are separated into "intrinsic" and "extrinsic" S-stars, based on direct observation of the Technetium line, or infrared properties.

The dust mass loss rate per unit distance is derived from IRAS 60 μm data, and the gas mass loss rate per unit distance is derived from CO data. Distances and luminosities are estimated, partly from HIPPARCOS parallax data. The S-stars without Tc have lower mass loss rates, than those with Tc.

It is shown that neglect of the stellar contribution to the observed 60 μm flux can lead to an overestimate of the dust mass loss rate.

Diagrams showing mass loss rate, dust-to-gas ratio and expansion velocity versus pulsation period are presented, and compared to similar data for carbon- and oxygen-rich Miras. The S-Miras do not stand out in any way from the C- or O-Miras in these diagrams. In the diagram with expansion velocity versus pulsation period, the S-SRs span the same range in velocity as the S-Miras, but they have periods which are about a factor of 2.5 shorter. This was previously noted for O-rich SRs (Kerschbaum et al. 1996, Kerschbaum & Olofsson 1998). As in that case, the most straightforward explanation seems to be that SRs pulsate in a higher order pulsation mode.

Acknowledgements. The observations were performed in 1991 when MG was at the astronomical institute "Anton Pannekoek" of the University of Amsterdam and whose research was supported under grant 782-373-030 by the Netherlands Foundation for Research in Astronomy (ASTRON), which is financially supported by the Netherlands Organisation for Scientific Research (NWO). An anonymous referee is thanked for her/his comments. This research has made use of the SIMBAD database, operated at CDS, Strasbourg, France.

References

Bieging J.H., Latter W.B., 1994, ApJ 422, 765
Bujarrabal V., Alcolea J., 1991, A&A 251, 536
Bujarrabal V., Planesas P., Martin-Ointado J., Gomez-Gonzales J., Del Romero A., 1986, A&A 162, 157
Claussen M.J., Kleinmann S.G., Joyce R.R., Jura M., 1987, ApJS 65, 385
Engels D., Lewis B.M. , 1996, A&AS 116, 117
Epchtein N., Le Bertre T., Lepine J.R.D., 1990, A&A 227, 82
Feast M.W., Glass I.S., Whitelock P.A., Catchpole R.M., 1989, MNRAS 241, 375
Fluks M.A., Plez B., Thé P.S., et al., 1994, A&AS 105, 311
Gezari D.Y., Schmitz M., Pitts P.S., Mead J.M., 1993, NASA Reference publication 1294
Grasdalen G., Gehrz R.D., Hackwell J.A., Castelaz M., Gullixson C., 1983, ApJ 553, 413
Groenewegen M.A.T., 1993a, A&A 271, 180
Groenewegen M.A.T., 1993b, Ph.D. Thesis, Chapter 5, University of Amsterdam
Groenewegen M.A.T., 1994, A&A 290, 531
Groenewegen M.A.T., 1997, in: "The impact of large-scale IR surveys", eds. F. Garzón et al., Kluwer Academic Publishers, p. 165
Groenewegen M.A.T., Baas F., de Jong T., Loup C., 1996, A&A 306, 241
Groenewegen M.A.T., Schrijver H., de Jong T., Slijkhuis S., 1997, in: "Hipparcos Venice '97", ed. B. Battrick, ESA SP-402, p. 323
Groenewegen M.A.T., Whitelock P.A., Smith C.H., Kerschbaum F., 1998, MNRAS 293, 18
Guglielmo F., Epchtein N., Le Bertre T., et al., 1993, A&AS 99, 31
Heske A, 1989, A&A 208, 77
Heske A, 1990, A&A 229, 494
Jorissen A., Knapp G.R., 1998, A&AS 129, 363 (JK)
Jorissen A., Frayer D.T., Johnson H.R., Mayor M., Smith V.V., 1993, A&A 271, 463
Jura M., 1987, ApJ 313, 743
Jura M., 1988, ApJS 66, 33
Jura M., Balm S.P., Kahane C, 1995, ApJ 453, 721
Jura M., Kleinmann S.G., 1992, ApJS 79, 105
Justtanont K., Skinner C.J., Tielens A.G.G.M., 1994, ApJ 435, 852
Kahane C., Barnbaum C., Uchida K., Balm S.P, Jura M., 1998, ApJ (June 10 issue)
Kastner J.H., 1992, ApJ 401, 337
Kerschbaum F., Olofsson H., 1998, in: "Proc. of the 23rd General Assembly of the IAU, eds. D.D. Sasselov and M. Takeuti, Universal Academy Press, inc., Tokyo, Japan, in press
Kerschbaum F., Olofsson H., Hron J., 1996, A&A 311, 273
Knapp G.R., Morris M., 1985, ApJ 292, 640
Little S.J., Little-Marenin I.R., Bauer W.H., 1987, AJ 94, 981
Loup C., Forveille T., Omont A., Paul J.F., 1993, A&AS 99, 291
Lutz T.E., Kelker D.H., 1973, PASP 85, 573
Mamon M., Glassgold A.E., Huggins P.J., 1980, ApJ 328, 797
Margulis M., van Blerkom D.J., Snell R.L., Kleinmann S.G., 1990, ApJ 361, 673
Mauersberger R., Guélin M., Martin-Pintado J., et al., 1989, A&AS 79, 217
Nyman L.-A., Booth R.S., Carlström U., et al., 1992, A&AS 93, 121
Olofsson H., Eriksson K., Gustafsson B., Carlström U., 1993, ApJS 87, 267
Olofsson H., Bergman P., Lucas R., et al., 1998, A&A 330, L1
Oudmaijer R.D., Groenewegen M.A.T., Schrijver H., 1998, MNRAS 294, L41
Sahai R., 1990, ApJ 362, 652
Sahai R., 1992, A&A 253, L33
Sahai R., Liechti S., 1995, A&A 293, 198
Smith V.V., Lambert D.L., 1988, ApJ 333, 219
Stephenson C.B., 1984, Publ. Warner and Swasey Obs. 3, 1
Stephenson C.B., 1990, AJ 100, 569
Van der Veen W.E.C.J., Olofsson H., 1990, in: "From miras to planetary nebulae", eds. M.O. Mennessier, A. Omont, editions Frontieres, Gif-sur-Yvette, p. 139
Van Eck S., Jorissen A., Udry S., Mayor M., Pernier B., 1998, A&A 329, 971
Volk K., Kwok S., 1988, ApJ 331, 435
Wannier P.G., Sahai R., 1986, ApJ 311, 335
Whitelock P.A., Menzies J., Feast M.W., et al., 1994, MNRAS 267, 711
Willems F.J., de Jong T., 1988, A&A 196, 173
Wood P.R., Bessell M.S., Fox M.W., 1983, ApJ 272, 99
Zijlstra A.A., Loup C., Waters L.B.F.M., de Jong T., 1992, A&A 265, L5
Zuckerman B., Dyck H.M., Claussen M.J., 1986, ApJ 304, 401